Electronic Supplementary Information

Droplet Energy Harvesting Panel

Xiaote XU, Pengyu LI, Yongtao DING, Wanghuai XU, Shiyuan Liu, Zhuomin Zhang, Zuankai Wang, Zhengbao YANG*

Department of Mechanical Engineering, City University of Hong Kong, Hong Kong SAR, China

Email: zb.yang@cityu.edu.hk

This file includes:

Other supplementary materials for the manuscript include the following:

Movies S1. Demonstration of hybrid Rain-Solar energy harvesting
Movies S2. Demonstration of self-powered wireless forest monitoring system

Supplementary Figures

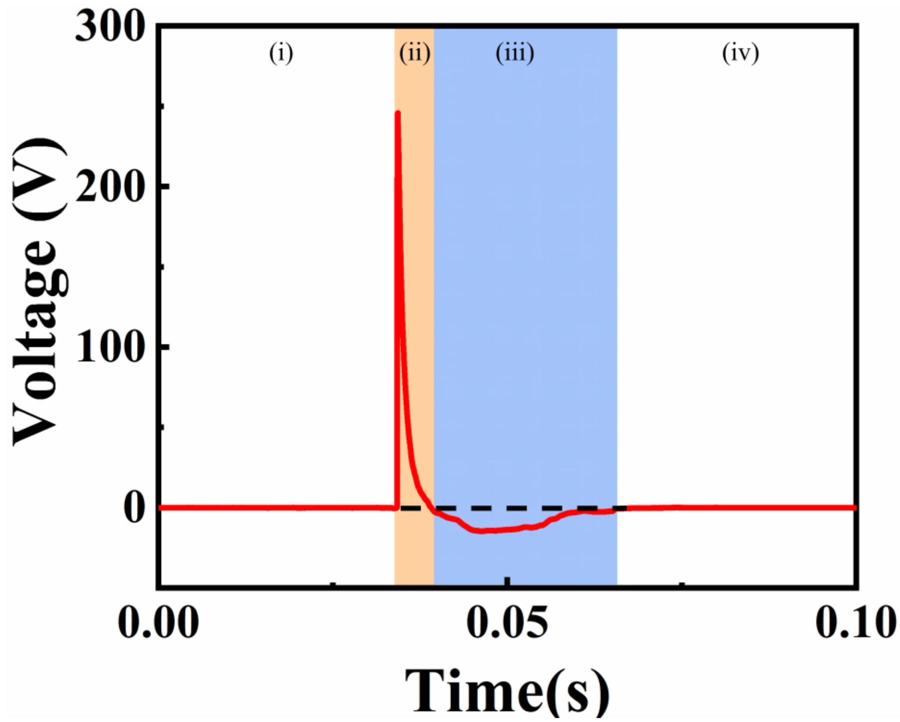

Figure S1. Time-resolved voltage waveform of DEH cell.

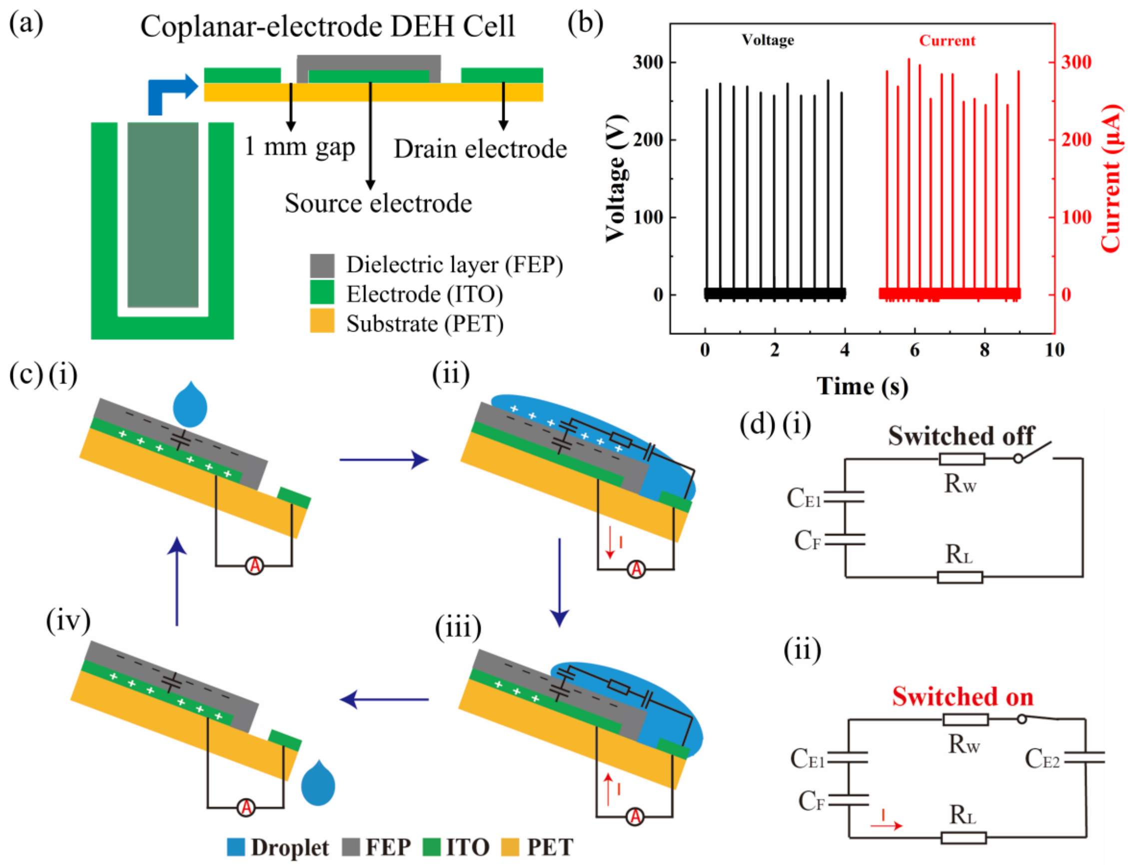

Figure S2. Coplanar-electrode DEH cell. (a) Top-view and side-view schematic diagram; (b) Open-circuit voltage and short-circuit current; (c) Working mechanism; (d) Equivalent circuit model, the parasitic capacitance is 0.26 pF, which is about 1/10 of the non-coplanar-electrode DEH cell and omitted in the schematic diagram.

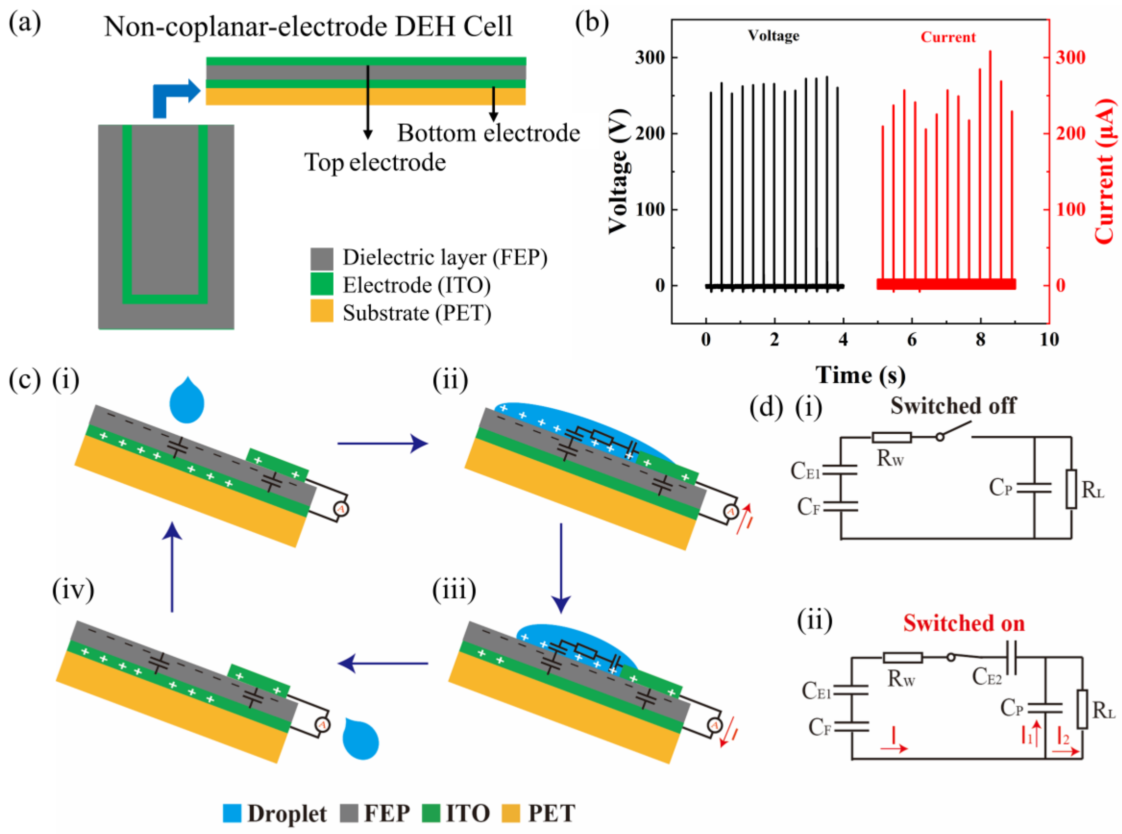

Figure S3. Non-coplanar-electrode DEH cell. (a) Top-view and side-view schematic diagram; (b) Open-circuit voltage and short-circuit current; (c) Working mechanism; (d) Equivalent circuit model, the parasitic capacitance C_P is 2.49 pF, which is about tenfold as the coplanar-electrode DEH cell (0.26 pF).

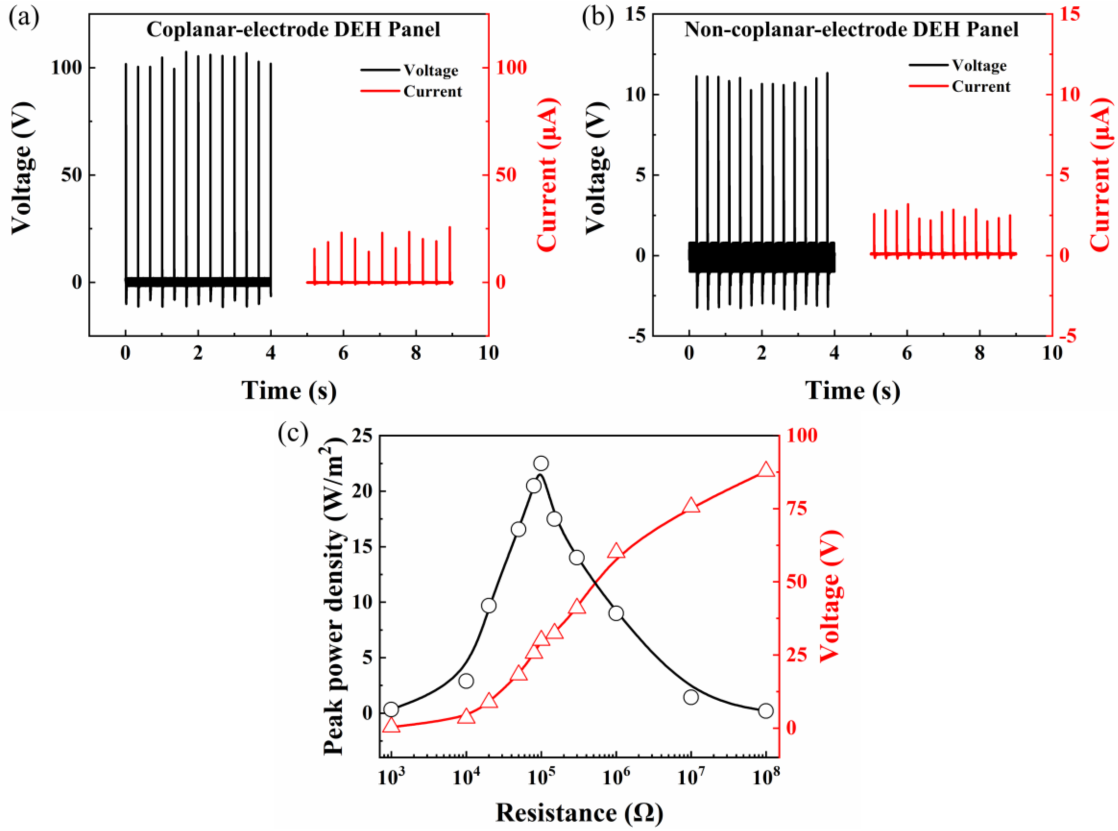

Figure S4. Large-area DEH panel. (a) Open-circuit voltage and short-circuit current of the coplanar-electrode DEH panel; (b) Open-circuit voltage and short-circuit current of the non-coplanar-electrode DEH panel; (c) Impedance matching of the coplanar-electrode DEH panel, the maximum power density of the coplanar panel is 22.52 W m^{-2} (at the load resistance of 100 kΩ).

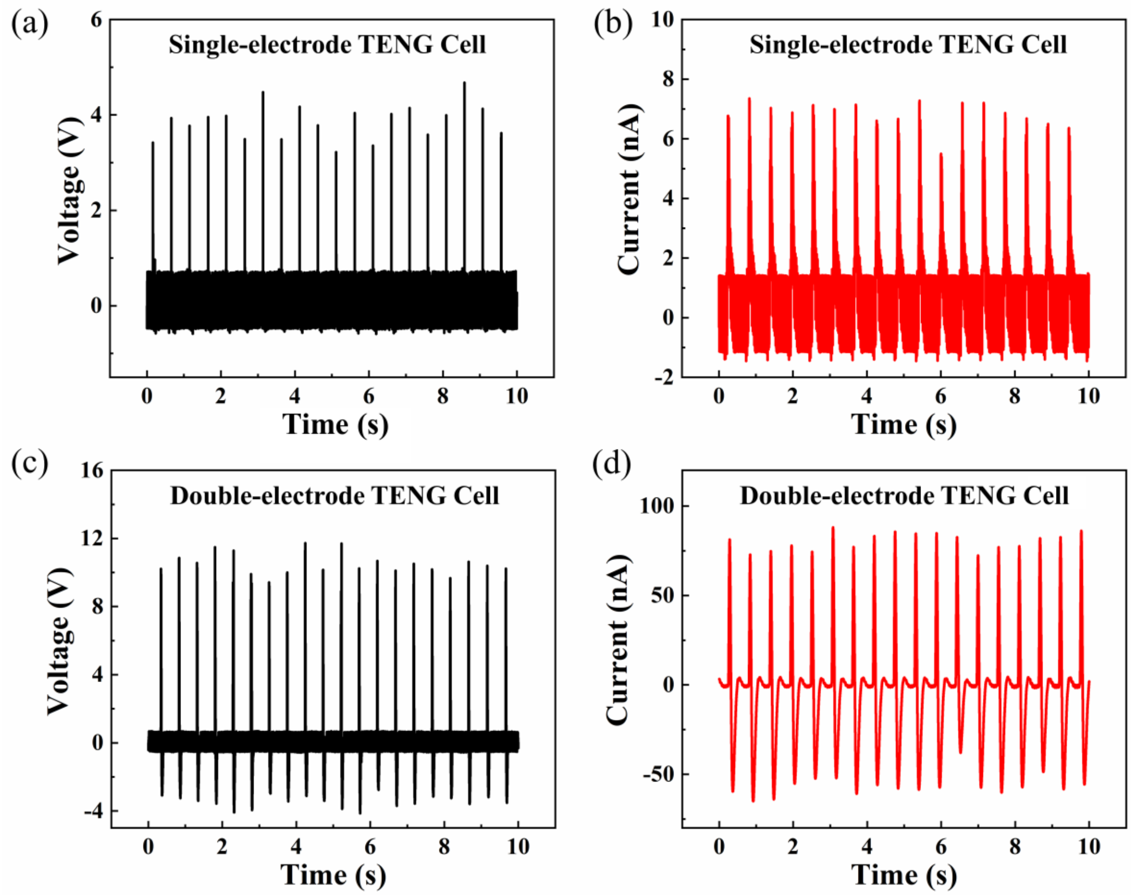

Figure S5. Liquid-solid TENG cells. (a) Open-circuit voltage of single-electrode TENG cell; (b) Short-circuit current of single-electrode TENG cell; (c) Open-circuit voltage of double-electrode TENG cell; (b) Short-circuit current of double-electrode TENG cell.

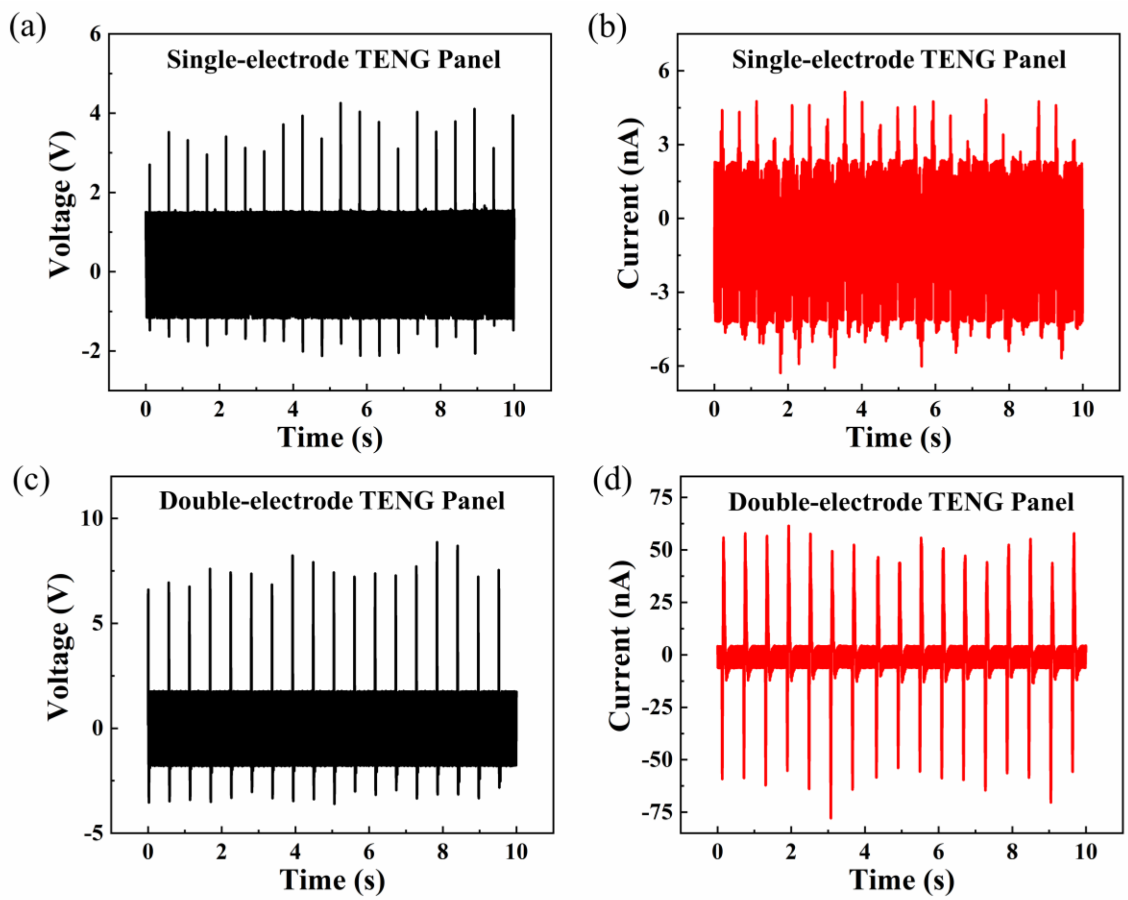

Figure S6. Large-area liquid-solid TENG panels. (a) Open-circuit voltage of single-electrode TENG panel; (b) Short-circuit current of single-electrode TENG panel; (c) Open-circuit voltage of double-electrode TENG panel; (b) Short-circuit current of double-electrode TENG panel.

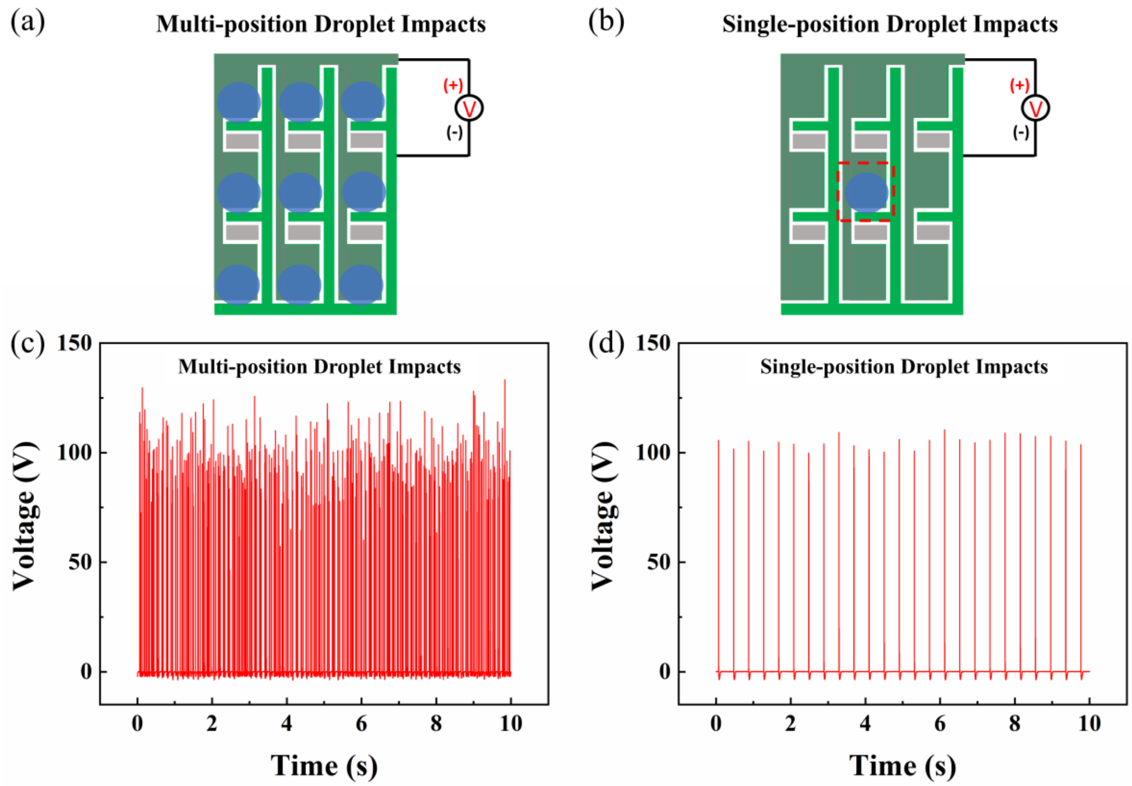

Figure S7. Large-area coplanar-electrode DEH panel for multi-position droplet impacts. (a) Schematics of large-area DEH panels under multi-position droplet impacts and (b) single-position droplet impacts; (c) Open-circuit voltages of large-area DEH panels under multi-position droplet impacts and (b) single-position droplet impacts.

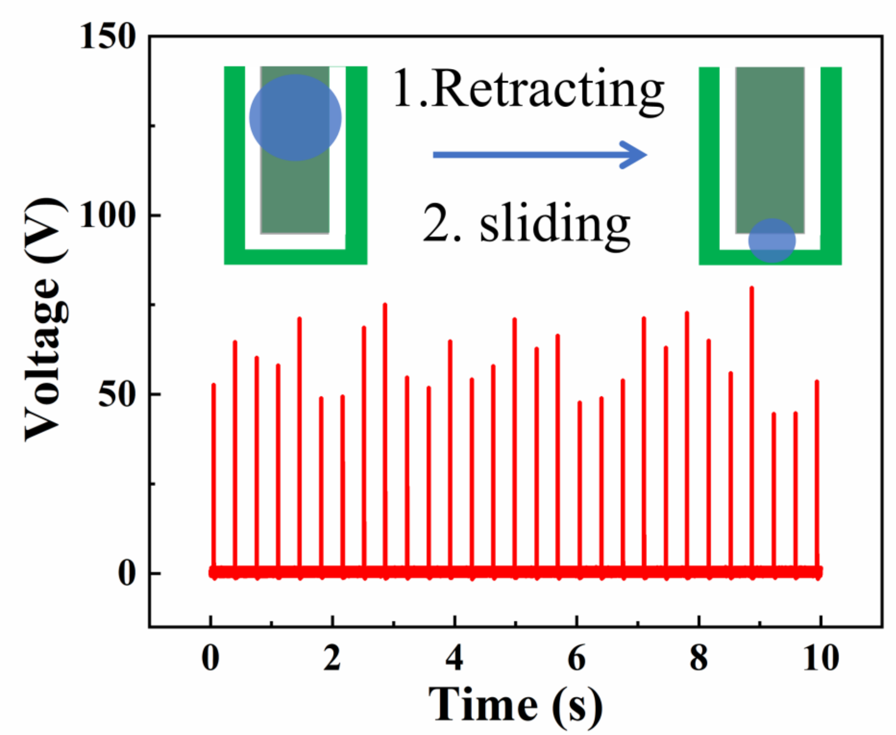

Figure S8. Schematic and output of the sliding contact.

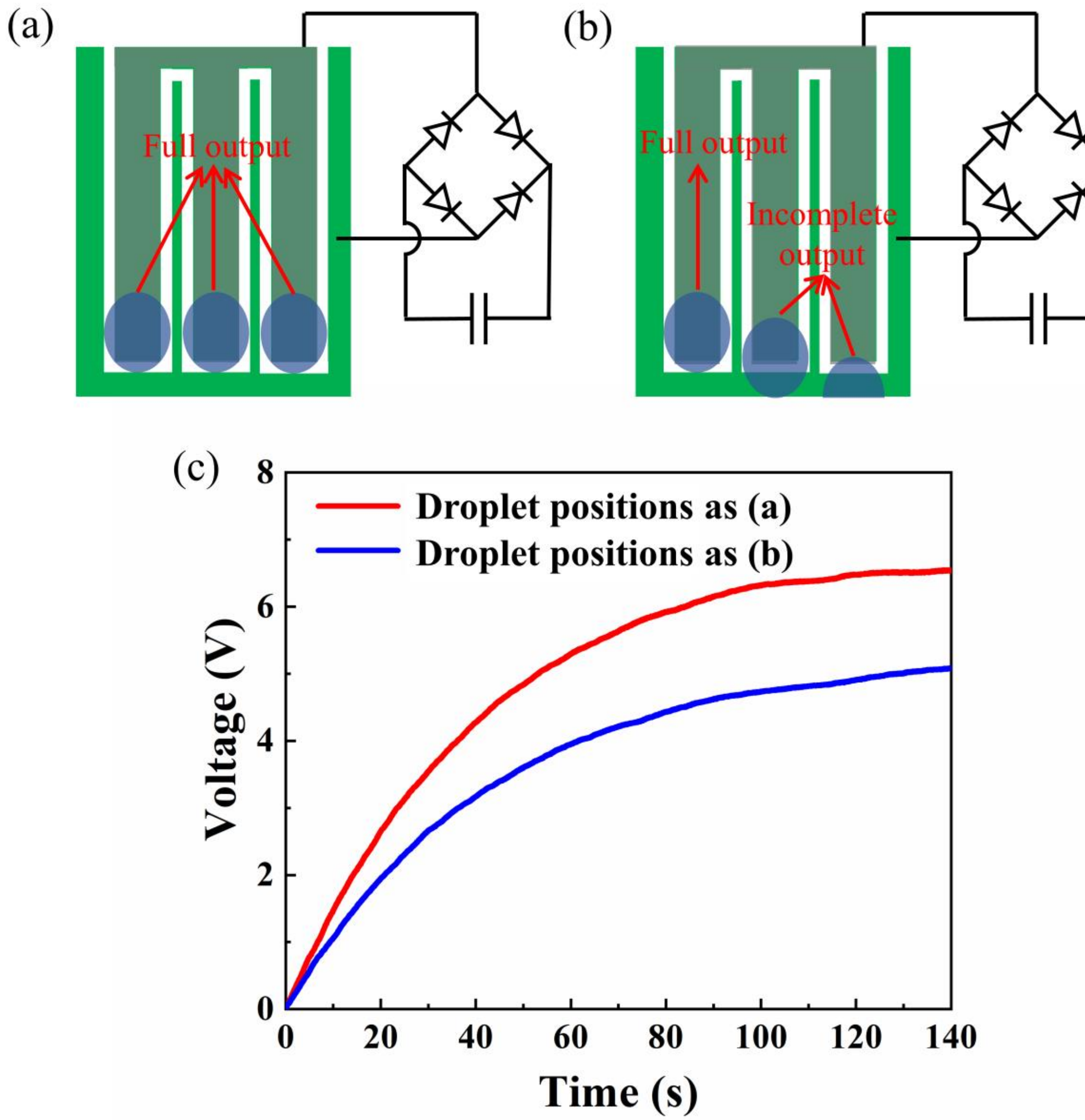

Figure S9. Schematic and charging performance of three different droplet impact positions. (a) Droplet impacts of three full outputs; (b) Droplet impacts of one full output and two incomplete outputs; (c) Comparison of charging performance, the charging curve shows that more full outputs contribute to higher charging performance.

(a) (b)

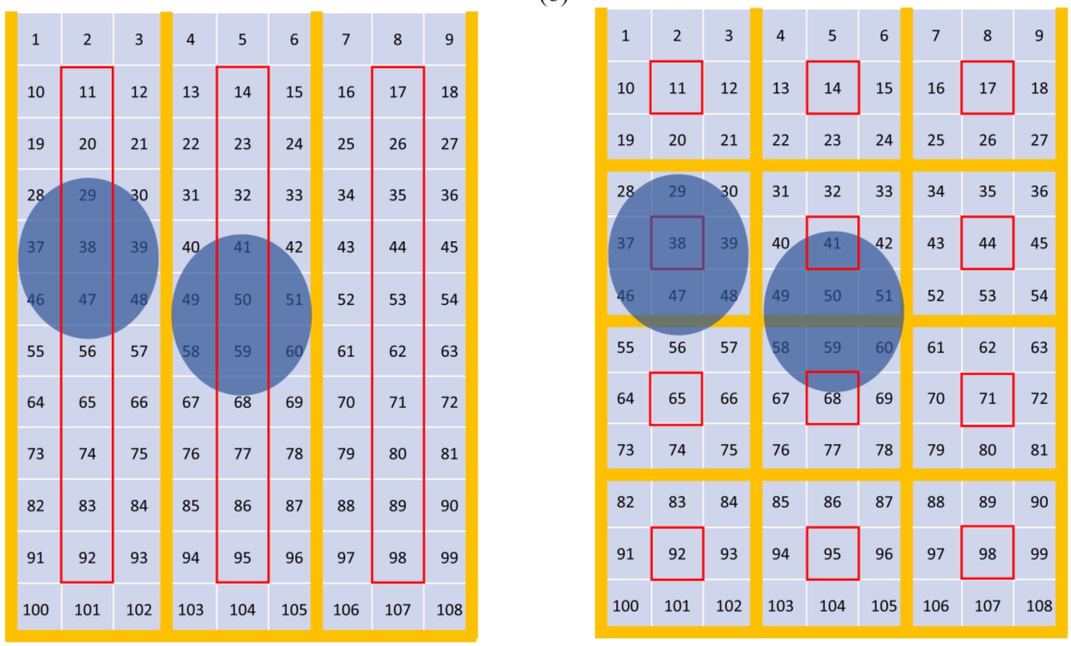

Figure S10. Theoretical possibility of full output for strip-like DEH panel and checker-like DEH panel. (a) The possibility of full output is 27.8% for the strip-like DEH panel; (b) The possibility of full output is 11.1% for the checker-like DEH panel, the possibility of full output for the strip-like DEH panel will be nearly 3 times the checker-like DEH panel when the Y-direction dimension becomes infinitely large.

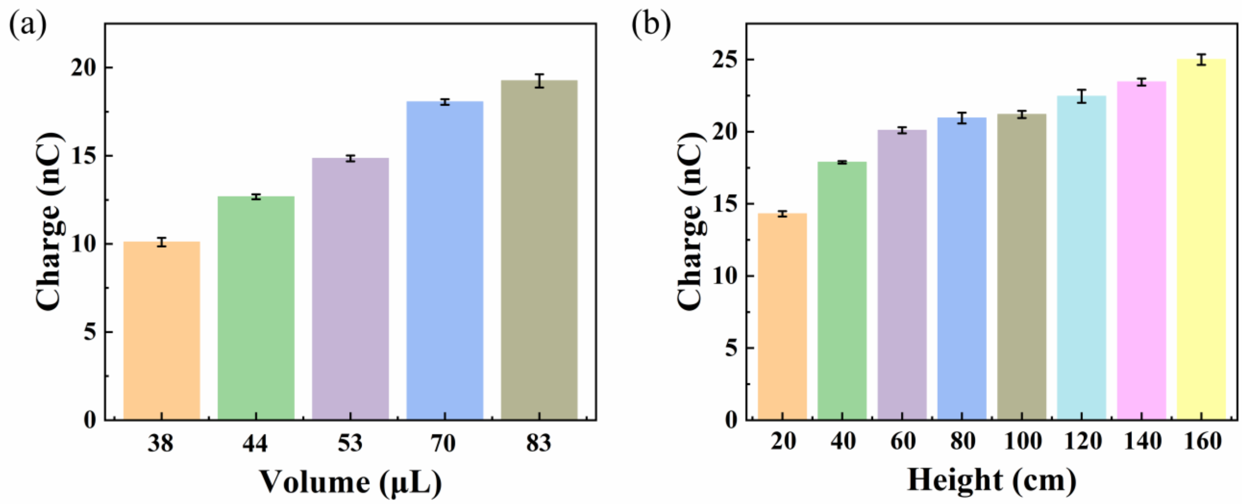

Figure S11. Effect of droplet volume and dripping height on the output. (a) Droplet volume from 38 μL to 83 μL; (b) Dripping height from 20 cm to 160 cm.

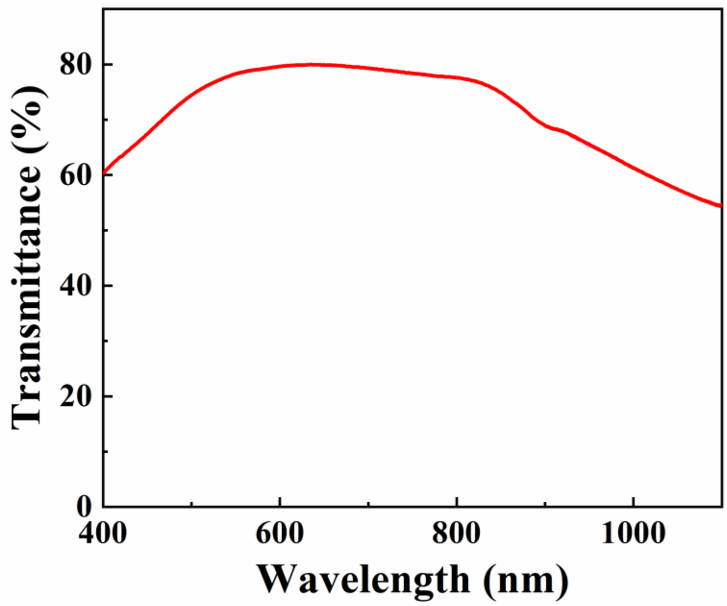

Figure S12. Transmittance spectrum of transparent DEH panel.

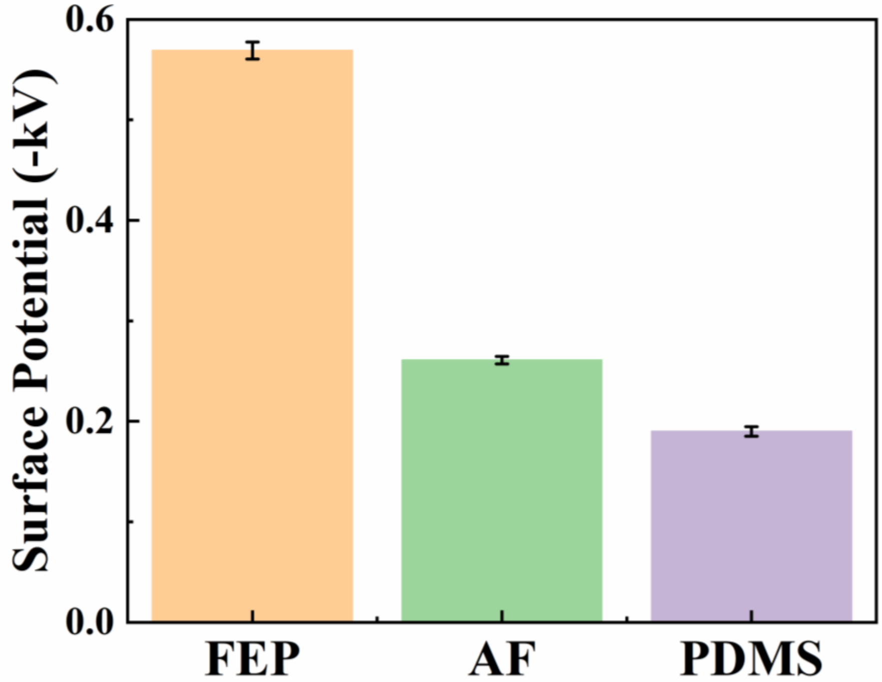

Figure S13. Surface potential of transparent dielectric materials.

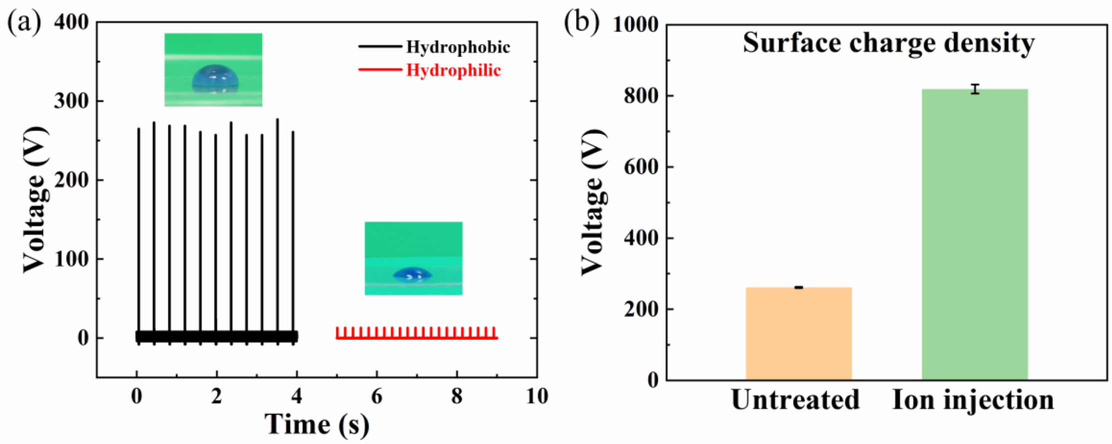

Figure S14. Effect of wettability and surface charge density on the output. (a) Hydrophobic surface (untreated) and hydrophilic surface (treated by air plasma); (b) Untreated and ion injection (treated by releasing the trigger of an antistatic gun Zerostat3 at a vertical distance of about 5.0 cm).

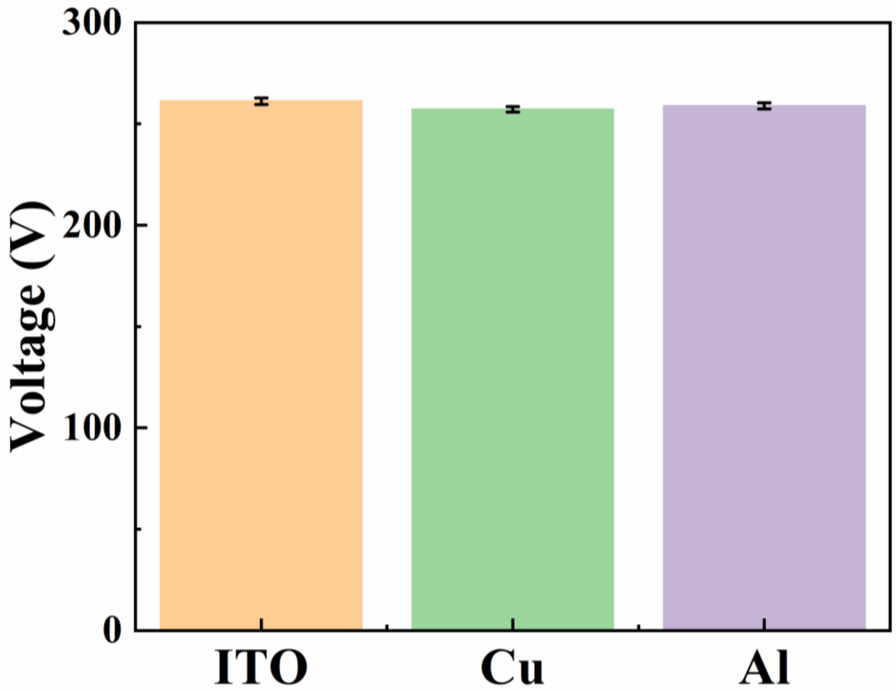

Figure S15. Effect of electrode materials on the output.

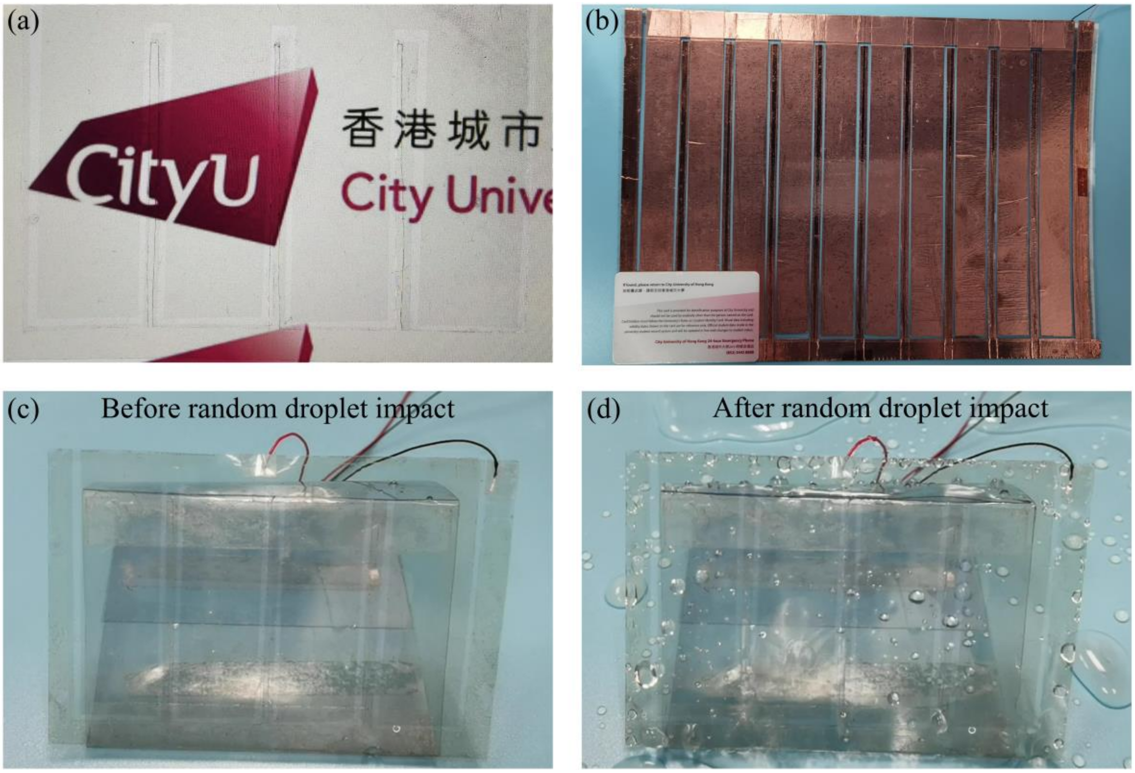

Figure S16. Optical image of coplanar-electrode DEH panels. (a) Transparent DEH panel (5.7 cm × 8.6 cm, credit-card-sized); (b) Large-area DEH panel (29.7 cm×21.0 cm, A4-paper-sized); (c) Before random droplet impact; (d) After random droplet impact.

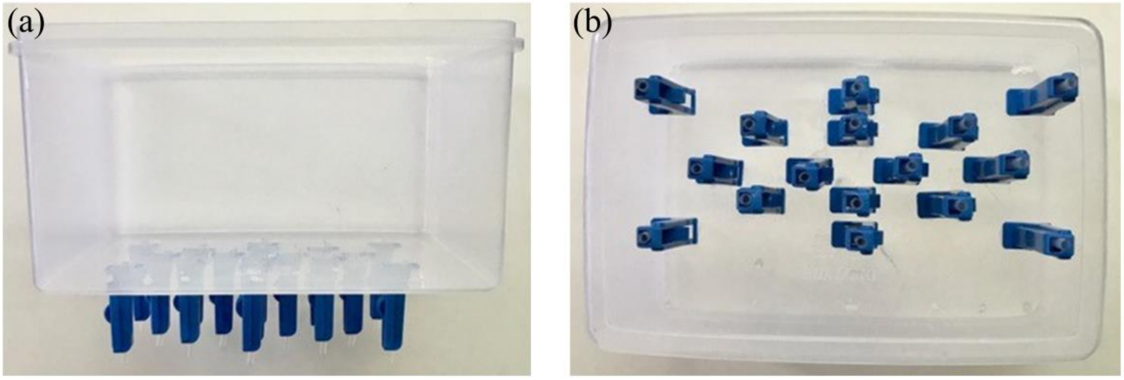

Figure S17. Optical image of setup for random droplet generation.

Supporting Tables

Table S1. Performance comparison of different cell devices and large-area panels.

Type	Device structure	Transferred charge (nC)	Voltage (V)	Current (μA)	Power density (W m^{-2})
Cell device	Single-electrode TENG	0.023	3.88	0.007	6.02×10^{-3}
	Double-electrode TENG	3.85	10.64	0.081	45.3×10^{-3}
	Non-coplanar-electrode DEH	14.3	261.5	246.1	75.84
	Coplanar-electrode DEH	14.85	266.6	273.6	83.02
Large-area panel (A4-paper-sized)	Single-electrode TENG	0.018	3.27	0.005	4.28×10^{-3}
	Double-electrode TENG	2.23	7.37	0.055	21.7×10^{-3}
	Non-coplanar-electrode DEH	4.58	10.76	2.75	46.3×10^{-3}
	Coplanar-electrode DEH	10.49	103.47	19.78	22.52

* The power density is calculated by the followed equation:
Power density = Power/droplet spreading area, the droplet spreading area is assumed as 2.5 cm^2.

Table S2. Performance comparison of the coplanar-electrode DEH cell with reported droplet energy harvesters.

Ref.	Device structure	Transferred charge (nC)	Voltage (V)	Current (μA)	Power density (W m^{-2})
Ref.[1]	Single-electrode TENG	1.5	9.3	17	0.58 *
Ref.[2]	Single-electrode TENG	1.5	52	43	1.31 *
Ref.[3]	Single-electrode TENG	0.6	7	0.128	1.08×10^{-3} *
Ref.[4]	Single-electrode TENG	-	30	27.5	1.81 *
Ref.[5]	Single-electrode TENG	-	13.6	3.2	0.14
Ref.[6]	Single-electrode TENG	0.8	9.2	8.7	-
Ref.[7]	Single-electrode TENG	-	2.86	1.8	0.013
Ref.[8]	Single-electrode TENG	1	30	10	9.6×10^{-3}
Ref.[9]	Single-top-electrode TENG	-	40.74	0.032	0.464*
Ref.[10]	Single-top-electrode TENG	2	68.1	84.8	-
Ref.[11]	Double-electrode TENG	2.2	0.175	0.018	4.87×10^{-6} *
Ref.[12]	Double-electrode TENG	2.76	5.48	0.177	1.19×10^{-3} *
Ref.[13]	Double-electrode TENG	5	0.055	0.005	-
Ref.[14]	Double-electrode TENG	-	18	14	0.8×10^{-3} *
Ref.[15]	Double-electrode TENG	3.18	11.8	0.78	-
Ref.[16]	Transistor-inspired structure	8.5	40	2.5	0.038
Ref.[17]	Transistor-inspired structure	8.89	23.92	2.41	0.68*
Ref.[18]	Transistor-inspired structure	30	37.11	7.56	0.59*
Ref.[19]	Transistor-inspired structure	13	60	9	0.072
Ref.[20]	Transistor-inspired structure	49.8	143	270	50.1
This work	Transistor-inspired structure	14.85	266.6	273.6	83.02

* The power density is calculated by the followed equation:
Power density = Power/droplet spreading area[20], the droplet spreading area is assumed as 2.5 cm^2.

Supporting Reference

1 Z. H. Lin, G. Cheng, S. Lee, K. C. Pradel and Z. L. Wang, *Adv. Mater.*, 2014, **26**, 4690–4696.
2 Z. H. Lin, G. Cheng, W. Wu, K. C. Pradel and Z. L. Wang, *ACS Nano*, 2014, **8**, 6440–6448.
3 S. B. Jeon, D. Kim, G. W. Yoon, J. B. Yoon and Y. K. Choi, *Nano Energy*, 2015, **12**, 636–645.
4 X. Liu, K. Cheng, P. Cui, H. Qi, H. Qin, G. Gu, W. Shang, S. Wang, G. Cheng and Z. Du, *Nano Energy*, 2019, **66**, 104188.
5 J. Xiong, M. F. Lin, J. Wang, S. L. Gaw, K. Parida and P. S. Lee, *Adv. Energy Mater.*, 2017, **7**, 1–10.
6 L. Li, X. Li, X. Yu, C. Shen, X. Wang, B. Li, J. Li, L. Wang, J. Yin and W. Guo, *Nano Energy*, 2022, **95**, 107024.
7 Q. Liang, X. Yan, X. Liao and Y. Zhang, *Nano Energy*, 2016, **25**, 18–25.
8 L. E. Helseth and X. D. Guo, *Renew. Energy*, 2016, **99**, 845–851.
9 R. G. Neo and B. C. Khoo, *Appl. Energy*, 2021, **285**, 116428.
10 N. Zhang, H. Gu, K. Lu, S. Ye, W. Xu, H. Zheng, Y. Song, C. Liu, J. Jiao, Z. Wang and X. Zhou, *Nano Energy*, , DOI:10.1016/j.nanoen.2020.105735.
11 B. Kil Yun, H. Soo Kim, Y. Joon Ko, G. Murillo and J. Hoon Jung, *Nano Energy*, 2017, **36**, 233–240.
12 W. Zhong, L. Xu, F. Zhan, H. Wang, F. Wang and Z. L. Wang, *ACS Nano*, , DOI:10.1021/acsnano.0c04413.
13 S. Hu, Z. Shi, R. Zheng, W. Ye, X. Gao, W. Zhao and G. Yang, *ACS Appl. Mater. Interfaces*, , DOI:10.1021/acsami.0c10097.
14 L. E. Helseth and X. D. Guo, *Smart Mater. Struct.*, , DOI:10.1088/0964-1726/25/4/045007.
15 W. Yuan, C. Zhang, B. Zhang, X. Wei, O. Yang, Y. Liu, L. He, S. Cui, J. Wang and Z. L. Wang, *Adv. Mater. Technol.*, 2021, **2101139**, 1–8.
16 Q. Zhang, C. Jiang, X. Li, S. Dai, Y. Ying and J. Ping, *ACS Nano*, 2021, **15**, 12314–12323.
17 C. Ye, D. Liu, X. Peng, Y. Jiang, R. Cheng, C. Ning, F. Sheng, Y. Zhang, K. Dong and Z. L. Wang, *ACS Nano*, 2021, **15**, 18172–18181.
18 L. Zhao, J. Duan, L. Liu, J. Wang, Y. Duan, L. Vaillant-Roca, X. Yang and Q. Tang, *Nano Energy*, 2021, **82**, 105773.
19 F. Liang, X. Chao, S. Yu, Y. Gu, X. Zhang, X. Wei, J. Fan, X. ming Tao and D. Shou, *Adv. Energy Mater.*, 2022, **12**, 1–10.
20 W. Xu, H. Zheng, Y. Liu, X. Zhou, C. Zhang, Y. Song, X. Deng, M. Leung, Z. Yang, R. X. Xu, Z. L. Wang, X. C. Zeng and Z. Wang, *Nature*, 2020, **578**, 392–396.